ANALYSES OF FLOW FIELD STRUCTURES AROUND LINEAR-TYPE AEROSPIKE NOZZLES USING LIF AND PSP

Tomohide Niimi, Hideo Mori, Kazuki Okabe, Yusuke Masai and Mashio Taniguchi
Department of Mechanical Engineering, Nagoya University
Furo-cho, Chikusa, Nagoya 464-8603, Japan

ABSTRACT

Aerospike nozzles have been expected as a candidate for an engine of reusable space shuttles to respond to growing demand for rocket-launching at the lower cost. In this study, the flow field structures in any cross sections around the linear-type aerospike nozzle are visualized and analyzed, using laser induced fluorescence (LIF) of NO seeded in the carrier gas N_2. Since the flow field structure is affected mainly by the pressure ratio (P_s/P_a), the linear-type aerospike nozzle is set inside the vacuum chamber to carry out the experiments in the wide range of pressure ratios from 75 to 250. Flow fields are visualized in several cross-sections, demonstrating the complicated three-dimensional flow field structures. Pressure sensitive paint (PSP) of PtTFPP bound by poly(TMSP) is also applied successfully to measurement of the complicated pressure distribution on the spike surface.

INTRODUCTION

To respond to growing demand for rocket-launching at the lower cost, aerospike nozzles[1] have been expected as candidates for engines of reusable space shuttles, which are required to have a simple mechanism and high performances from the ground to high altitude. Since the aerospike nozzle expands the combustion gases equilibrating with the ambient pressure, the nominal expansion ratio is adjusted automatically to the suitable one at any altitude. Though the aerospike nozzle becomes longer than the bell-shaped nozzle with the same expansion ratio, it has been reported that, even if the spike is shortened, the reduction of the nozzle thrust is negligibly small because of the compensation for the thrust loss by the base pressure[2]. So far, the flow fields of the annular- or linear-type aerospike nozzles have been studied mainly by computer simulations[2], because large ratios of the source pressure (P_s) to the ambient one (P_a) are difficult to be achieved experimentally at the ground. In some experiments, the flow fields are visualized by Schlieren method[3], but the local information cannot be obtained because this method is based on change of refractive index along the line of sight.

Since the flow field structure is affected mainly by the pressure ratio (P_s/P_a), in this study, we set a linear-type aerospike nozzle in a vacuum chamber to carry out the experiments in the wide range of pressure ratios and then clarify the complicated flow field structures around the linear-type aerospike nozzle. To visualize and analyze the flow field structure in any cross sections around the linear-type aerospike nozzle, laser induced fluorescence (LIF) of NO seeded in the carrier gas N_2 is employed. LIF is not only a non-intrusive measurement technique, but can also visualize the flow field structure in any cross-sections unlike the Schlieren method. We also apply pressure sensitive paint (PSP) of PtTFPP bound by poly(TMSP)[4] to measure the complicated pressure distribution on the spike surface.

EXPERIMENTS

Visualization of Jet Structures using NO-LIF

Figure 1 shows a schematic diagram of the experimental apparatus used in this study to visualize flow fields of jets issued from linear-type aerospike nozzles. A broadband ArF excimer laser (Lambda Physik LPX 105E; wavelength 193 nm, FWHM 0.5nm) is used as an excitation source. The laser beam has pulse energy of typically 90mJ with 15ns pulse width and excites the transition (J''=23.5–34.5) in the $B^2\Pi^+ \leftarrow X^2\Pi$ (7,0) band and that of (J''=15.5–46.5) in the $D^2\Sigma^+ \leftarrow X^2\Pi$ (0,1) band of NO near 193nm. The laser beam propagates to an expansion chamber by mirrors and then turns into a 0.3-mm-thick and 20-mm-high laser sheet by a fused silica cylindrical lens (400-mm focal length). The beam waist area of the laser sheet is used to visualize the flow field. Nitrogen gas premixed with 1% nitric oxide in a reservoir kept at room temperature is expanded through the linear-type aerospike nozzle into the expansion chamber evacuated by a rotary pump. The flow field in the region of 20 mm × 14 mm is imaged onto an image-intensified CCD camera (Hamamatsu C7300-10) set perpendicular to the laser sheet. Resolution of the CCD camera is 1280 × 1024 pixels and 4096 gray levels. We synchronize the CCD camera with a laser pulse and use a UG5 filter, to eliminate elastically scattered laser light and to pass most of broadband NO fluorescence. The steadiness of flow field allows us to accumulate the image data for three laser shots, and the final images are stored in a personal computer. The cylindrical lens and the CCD camera are set on pulse stages and a distance between the laser sheet and the camera is kept constant, enabling to visualize the flow fields at any cross sections.

0-7803-8149-1/03/$17.00©2003 IEEE

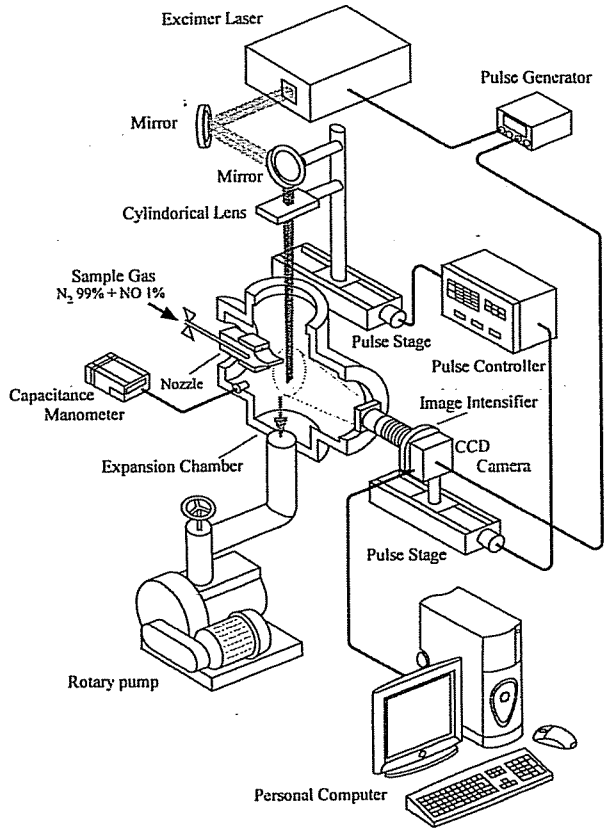

Figure 1 Experimental Apparatus

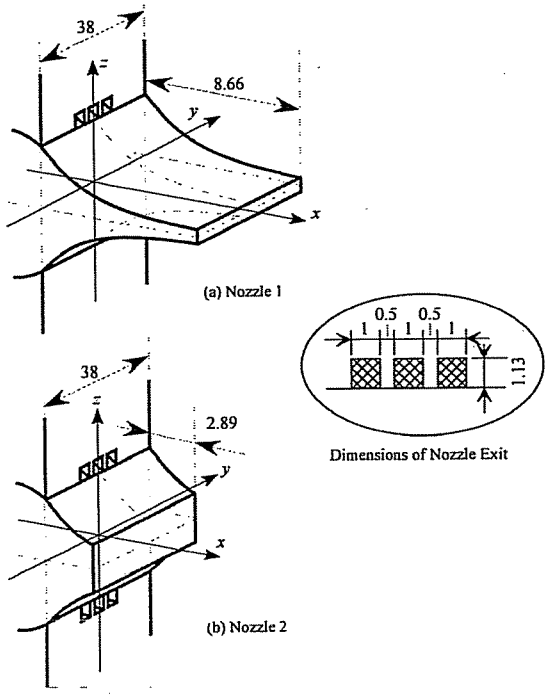

Figure 2 Aerospike Nozzles

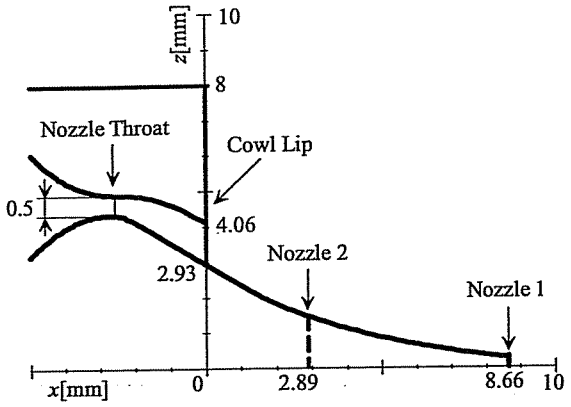

Figure 3 Cross Sectional View of the Aerospike Nozzles

Measurement of pressure distribution on nozzle surfaces

To measure the pressure distribution on the nozzle surface, we apply the PSP of PtTFPP/poly(TMSP) which has high pressure sensitivity even in the rarefied gas flow[4]. In the experiments, pure oxygen gas is used to increase the pressure sensitivity. A xenon-arc lamp (Ushio UXL-500SX) with a band-pass filter is used as an excitation light source, and the light is transmitted via an optical fiber to illuminate the nozzle in the vacuum chamber. The wavelength range of the band-pass filter is 400±10 nm, which covers the absorption spectrum of PtTFPP/poly(TMSP). The luminescence is filtered by a long-pass filter (600 nm) to eliminate the light from the xenon lamp, and is detected by the CCD camera.

Design of the Aerospike nozzle

The linear-type aerospike nozzle used in this study is designed for two regions, i.e., inner nozzle region from source chamber to a rectangular jet orifice including a cowl lip and external expansion region from the jet orifice to a spike edge[5], assuming that all expansion processes are isentropic. The ratio of the cross section at the nozzle throat to that at the nozzle edge is set at 8.117 and the specific heat ratio at 1.4 because carrier gas consists of diatomic molecules. In this case, a jet boundary parallel to the nozzle centerline (x-axis) is formed at $P_s/P_a = 100$ (P_s is the source pressure and P_a is the ambient pressure).

Figure 2 shows the nozzles designed in this study, which have the cross section as shown in Fig. 3. The coordinate system is also depicted both in Figs. 2 and 3, in which the plane including the cowl lip is defined as the yz-plane and the line perpendicular to the yz-plane and passing through the center of the base plane is defined as the x-axis.

As shown in Fig. 2, nozzle 1 has three rectangular nozzle orifices in one side of the spike and width and

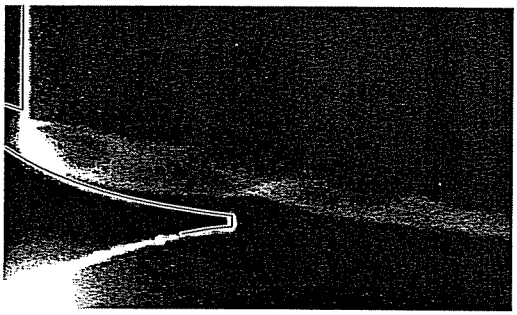

$P_s/P_a = 82.6$

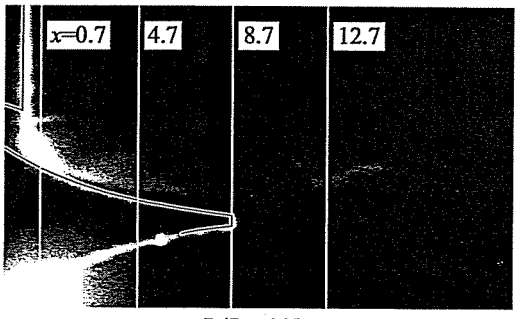

$P_s/P_a = 145$

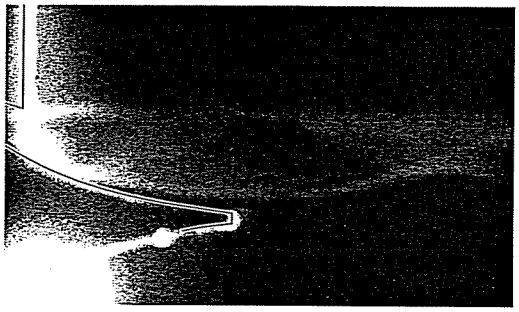

$P_s/P_a = 250$

Figure 4 LIF Image on xz-plane (Nozzle 1)

height of each orifice are 1 mm and 1.13 mm (0.5 mm at the throat), respectively. Interval of the centers of adjacent jet orifices is 1.5 mm as shown in an enlarged illustration. The spike of the nozzle 1 is truncated to 60 % (8.66 mm) of the entire length of the nozzle as shown in Fig. 3.

Nozzle 2 has jet orifices in the both sides of the spike, and each side has three orifices. The nozzle is used for experiments to examine the flow field structures interacting downstream with each other and the compensation for the thrust loss by the base pressure. The arrangement of the orifices of nozzle 2 is the same as nozzle 1 but the spike is truncated to 20 % (2.89 mm).

RESULTS AND DISCUSSION

Flow field structures along the spike

The structures of the adjacent jets interacting with each other on the one side of the spike of the nozzle 1 are visualized by the use of NO-LIF. Figure 4 shows the visualized images of the flow field in the xz-plane. The source pressure P_s is fixed at 88 kPa (660 Torr)

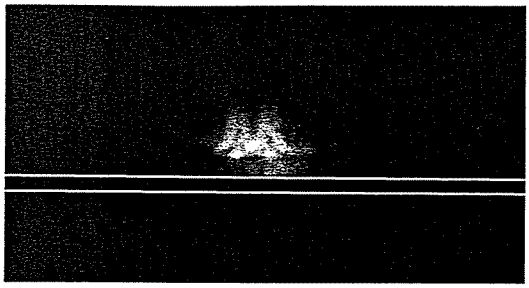

$x = 0.7$mm

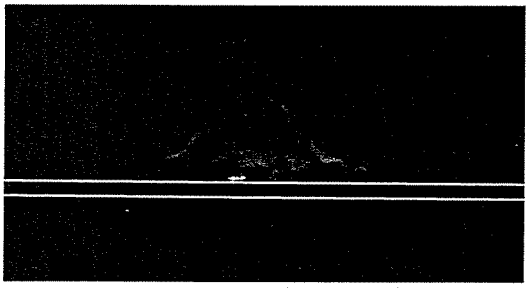

$x = 4.7$mm

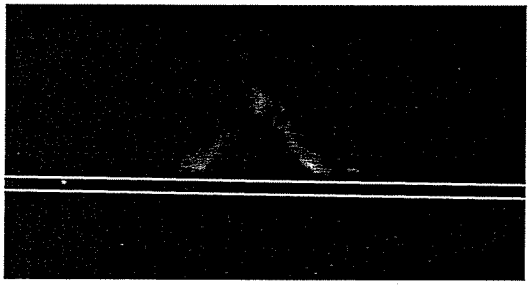

$x = 8.7$mm (near the base surface)

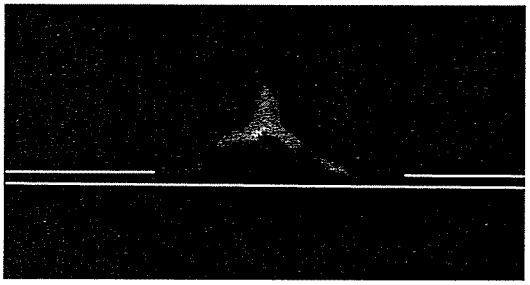

$x = 12.7$mm

Figure 5 LIF Image on yz-plane (Nozzle 1, P_s/P_a=145)

and P_s/P_a is set at 82.6, 145 and 250 by changing the ambient pressure P_a. It is found from these figures that the jets grow as P_s/P_a increases but no separation from the spike surface appears for any P_s/P_a, demonstrating the optimum nozzle design with small thrust loss.

Figure 5 is the visualized images in the planes parallel to the yz-plane at $P_s/P_a = 145$, which are indicated by white lines in a middle figure of Fig. 4. At the cross section just behind the nozzle exit ($x = 0.7$ mm), there appear two bright rectangular regions, corresponding to high-density regions due to the interaction of the

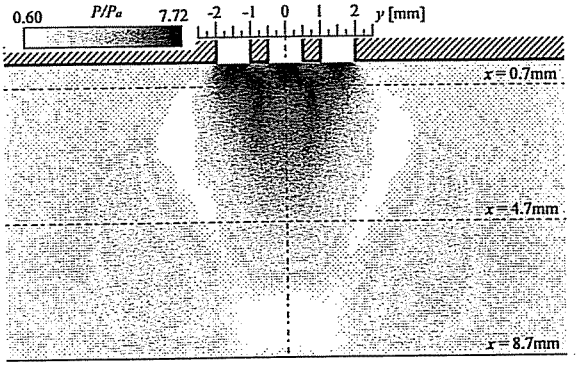

Figure 6 PSP Image on the Spike (Nozzle 1, P_s/P_a=145)

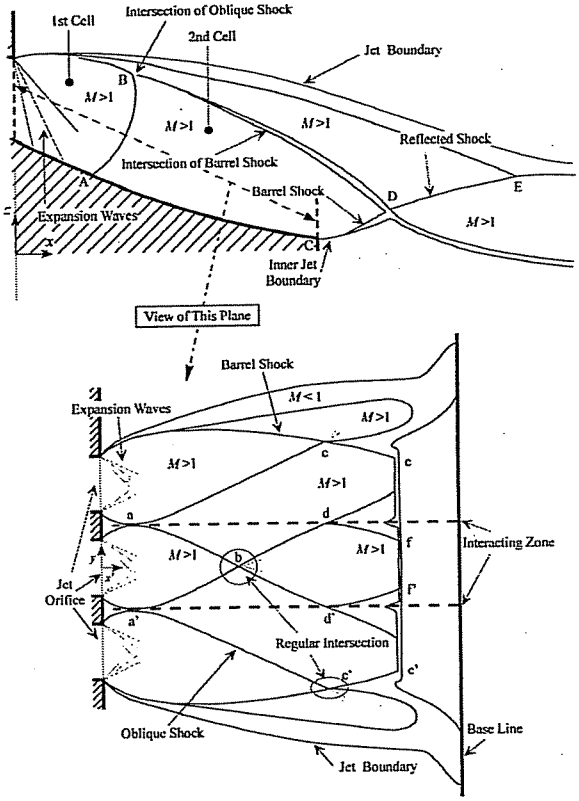

Figure 7 Jet Structure of Nozzle 1 (P_s/P_a=145)

adjacent jets. The pressure of these regions becomes relatively high, so that the gas expands again from here toward the z-direction. Since the pressure of the region between the two high-density regions becomes lower, the high-density regions move closer to each other gradually as the flow proceeds downstream and coalesce finally. As a result, the three jets issued from rectangular jet orifices turn into a triangle shape at $x = 4.7$ mm. The jets issued from the nozzle orifices in the both ends expand not only to the flow direction but also along the y-axis, so that the planar flows along the y-axis can be found. After passing through the base plane ($x = 8.7$mm), therefore, the flow field turn into an inversed Y-shape structure originated from a symmetrical point at which z- and y-component of the velocity balances.

Figure 6 shows a pressure distribution on the spike surface of the nozzle 1 at $P_s/P_a = 145$, measured by PSP. As shown in a gray scale in Fig. 6, white and black regions correspond to low and high pressure ones, respectively. In addition to three high-pressure regions ($y = 0$ and ± 1.5 mm) just behind the nozzle exits, there appear two high-pressure regions ($y = \pm 0.75$ mm). These are caused by the interaction of adjacent two jets, as mentioned above.

The flow field structures obtained from the above-mentioned analyses are shown schematically in Fig. 7 in which the upper figure indicates the flow field structure in the cross section at $y = 0$ and the lower one shows a view of the cross section depicted by the broken line in the upper figure. In the lower figure, the x' axis is defined in the direction of the downstream. The barrel shock waves originated from the edges of the nozzle exits reflect at the points a and a', and turn into the barrel shock waves ab and $a'b$ which intersect regularly at the point b corresponding to the curve AB shown in the upper figure. It is worthwhile to mention that the two high-pressure regions observed in Fig. 6 coincide with the regions just behind the points a and a', where the gas is compressed by the shock waves. The curve CD is a barrel shock wave originated from the spike edge and pressure in a region just behind the intersection D of the barrel shock waves CD and BD increases as shown in Fig. 4. As an increase in P_s/P_a, the jets grow self-similarly and a distance from the nozzle exit to the point D becomes longer.

Entire Flow field structures around the linear-type aerospike nozzle

Interactions of jets expanding from both sides of the spike are examined by using the nozzle 2. Figure 8 shows visualized images of the flow field in the xz-plane ($y = 0$), taken at $P_s/P_a = 75$, 125 and 169 and $P_s = 100$ kPa (750 Torr). It is found that, in the case of a larger value of $P_s/P_a = 169$, barrel shock waves originated from the spike edge interact with each other just behind the base. In this case, a back-flow from the interacting region toward the base may occur to compensate the thrust loss due to the truncation of the spike. On the other hand, in the case of low P_s/P_a of 75.0, the jets become small and weakly interact with each other behind the base, leading to no effective compensation of the thrust loss as mentioned above.

Visualized images of the jets at $P_s/P_a = 125$, taken at cross sections parallel to the yz-plane, are shown in Fig. 9. At the cross section just behind the nozzle exit, bright rectangular regions appears at $x = 1$ mm and the flow field turns into triangle shape at $x = 2.8$ mm as mentioned in the previous section.

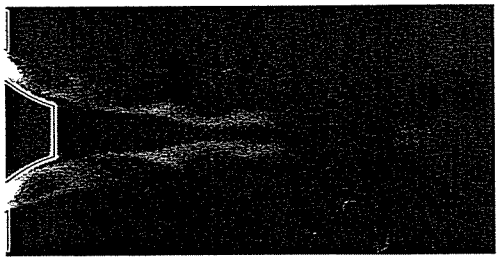

$P_s/P_a = 75.0$

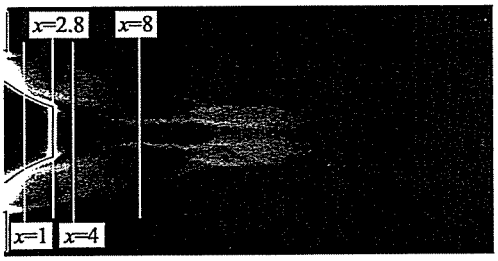

$P_s/P_a = 125$

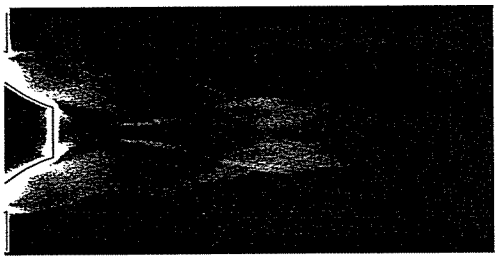

$P_s/P_a = 169$

Figure 8 LIF Image on xz-plane (Nozzle 2)

The interacting jets in the triangle shape expand into both of the y- and z-directions and turn into a shape like a cross as shown in the picture for $x = 8$ mm.

Schematic flow field structures for the nozzle 2 are shown in Fig. 10, in which the upper figure indicates the flow field structure in the cross section at $y = 0$ and the lower one shows a view of the cross section depicted by the broken arrow in the upper figure. The curves AB and BE correspond to the regular intersection of the barrel shock waves (correspond to the point b in the lower figure). The barrel shock wave CD originated from the spike edge reflects at the interacting point D and forms the barrel shock wave DE. Three shock waves intersect at the point E and the reflected shock wave EF emerges, which makes the Mach reflection together with another reflected shock wave $E'F'$ and forms the normal shock wave FF' at the downstream.

We also tried to measure a pressure distribution on the base by the use of PSP but could not confirm a pressure increase due to the back-flow in the range of P_s/P_a from 75.0 to 169. As shown in Fig. 8, we also found from the LIF images that the jets issued from the both side nozzles interact strongly just behind the base, but did not find the back-flow itself. This may

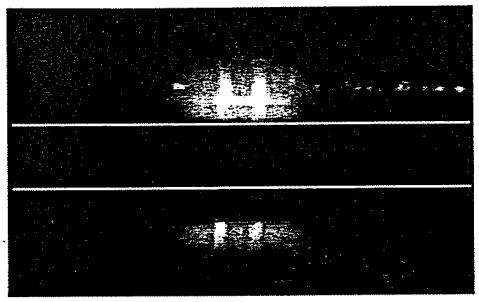

$x = 1$mm

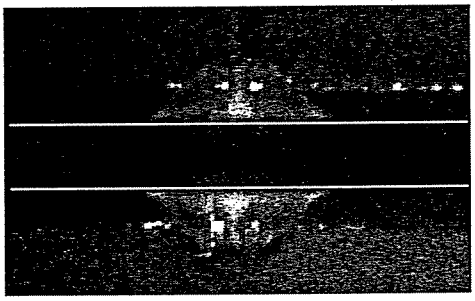

$x = 2.8$mm (near the base surface)

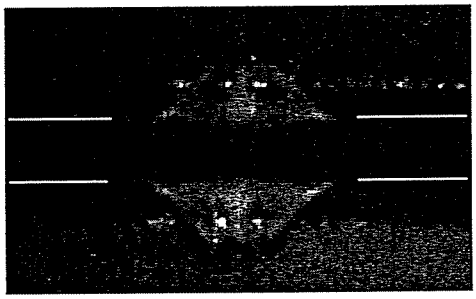

$x = 4$mm

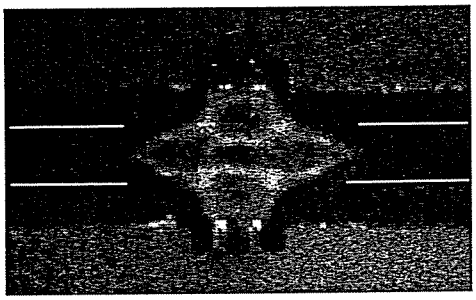

$x = 8$mm

Figure 9 LIF Image on yz-plane (Nozzle 2, P_s/P_a=125)

be caused by an expansion of the jets into the y-direction because of the small width of the nozzle and no sidewalls. Since a real aerospike nozzle has many jet orifices and large width, however, it may be considered that an effect the expansion into the direction of the y-axis becomes small.

CONCLUSION

We have applied a visualization method based on NO-LIF technique to analyses of structures of jets

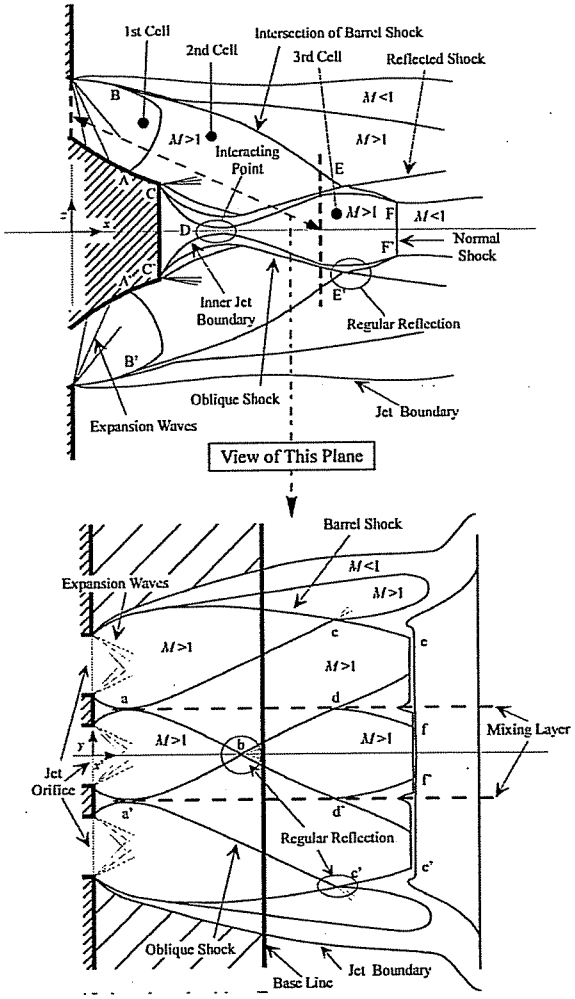

Figure 10 Jet Structure of Nozzle 2 (P_s/P_a=125)

around linear aerospike nozzles. PSP technique is also applied to measurements of pressure distributions on the nozzle surfaces. Concluding remarks are as follows:

1. We have enabled to visualize the jets of the aerospike nozzles at any cross sections by NO-LIF technique, and clarified the three-dimensional structures, depending on the length of the spike and the pressure ratio.
2. Expansion process around the aerospike nozzles is clarified by the visualized images in the cross sections parallel to the *yz*-plane. Strong expansion to the *z*-direction occurs from the high-density regions due to the interaction of the adjacent jets. Expansion to the *y*-direction in the downstream also occurs, leading to an inversed Y-shape structure.
3. The pressure distribution on the spike surface is obtained by PSP, showing a complicated pattern caused by the interaction of the adjacent jets.
4. Interactions of jets expanding from both sides of the spike are analyzed to examine the backflow. For high pressure ratio, the both jets interact strongly with each other just behind the base surface of the nozzle. Although the backflow itself has not been detected yet, it seems that the backflow from the interacting point to the base surface is generated, leading to compensation of the thrust. On the other hand, for low pressure ratio, the both jets do not interact with each other, and there seems to be no thrust yielded by the backflow.

The present work was supported by the Special Coordination Funds "Molecular Sensors for Aero-Thermodynamic Research (MOSAIC)", a grant-in-aid for Scientific Research of Ministry of Education, Culture, Sports, Science and Technology, and the Hibi Science Foundation. The authors would like to thank Prof. Kozo Fujii of the Institute of Space and Astronautical Science (ISAS) for his helpful advice. We also thank Mr. Yukihiro Nakanishi, a technical assistant of Nagoya University, for producing the aerospike nozzles used in this study.

REFERENCES

1) Rao, G.V.R., 1961, "Spike Nozzle Contour for Optimum Thrust", *Ballistic Missile and Space Technology*, Pergamon Press, Vol. 2, pp. 92-101.

2) Ito, T. and Fujii, K., 2003, "Flow Field and Performance Analysis of an Annular-Type Aerospike Nozzle with Base Bleeding", *Trans. Japan Soc. Aero. Space Sci.*, **46**-151, pp. 17-23.

3) Tomita, T., Takahashi M., and Onodera, T., 1998, "Visualization of Shock Wave Interaction on the Surface of Aerospike Nozzles", *34th AIAA/ASME/SAE/ASEE Joint Propulsion Conference & Exhibit*, AIAA 98-3523.

4) Mori, H. et al., 2003, "Application of PSP in low pressure regime", Proceedings of ICIASF'03 (in this book).

5) Lee, C. and Thompson, D., 1964, "Fortran Program for Plug Nozzle Design", NASA TM X-53019.